Materials & Design 227 (2023) 111783

Contents lists available at ScienceDirect

Materials & Design

journal homepage: www.elsevier.com/locate/matdes

A Self-healable, recyclable and degradable soft network structure material for soft robotics

Rui Chen [a,*], Xin Li [a], Qin Xiong [b], Xinyu Zhu [a], Huigang Wang [a], Wenbiao Wang [c], Guanjun Bao [c], Zhen Chen [d], Changyong (Chase) Cao [d,e,f], Jun Luo [a,g]

[a] State Key Laboratory of Mechanical Transmissions, Chongqing University, Chongqing 400044, China
[b] Southwest China Research Institute of Electronic Equipment, Chengdu 610036, China
[c] College of Mechanical Engineering, Zhejiang University of Technology, Zhejiang 310014, China
[d] Department of Mechanical and Aerospace Engineering, Case Western Reserve University (CWRU), Cleveland, OH 44106, USA
[e] Department of Electrical, Computer, and Systems Engineering, Case Western Reserve University, Cleveland, OH 44106, USA
[f] Advanced Platform Technology (APT) Center, Louis Stokes Cleveland VA Medical Center, Cleveland, OH 44106, USA
[g] School of Mechatronics Engineering and Automation, Shanghai University, Shanghai 200444, China

HIGHLIGHTS

- A self-healable, recyclable, and degradable soft material (SRDSM) with a network structure is studied.
- The SRDSM can withstand fracture stress of 3–4 MPa and be stretched 300 %-400 %.
- The SRDSM can recover 90% and 95% of its original mechanical properties after healing and recycling, respectively.
- With an SRDSM-based soft gripper made, the SRDSM can be applied in the field of soft robots.

GRAPHICAL ABSTRACT

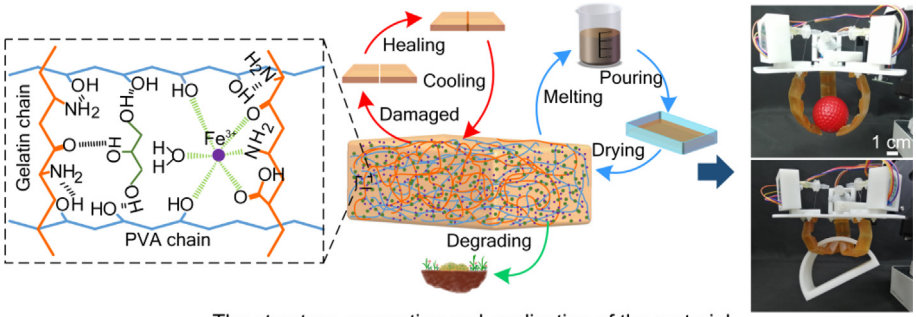

The structure, properties and application of the material

ARTICLE INFO

Article history:
Received 17 August 2022
Revised 19 January 2023
Accepted 20 February 2023
Available online 21 February 2023

Keywords:
Soft material
Self-healable
Recyclable
Degradable
Soft robots
Soft gripper

ABSTRACT

Soft materials enable soft robots to accommodate unstructured working environments robustly. However, they may be easily damaged and destroyed due to their weak mechanical properties. Moreover, most soft materials are not repairable or degradable after being broken or abandoned, resulting in new environmental burdens. Here, a self-healable, recyclable, and degradable soft material (SRDSM) with a network structure formed with gelatin and polyvinyl alcohol (PVA) is reported. The SRDSM exhibits a fracture strength of 3–4 MPa and a stretchability of up to 300 %-400 % by controlling the composition ratio and drying time. Results show that the SRDSM can recover 90 % of its original mechanical strength after healing and 95 % after recycling. An SRDSM-based soft gripper is demonstrated that can be self-healed under thermal cycling after minor damage. It can be recycled and remanufactured to restore its original functionality after severe damage. Furthermore, the soft gripper can decomposes and degrades entirely after contact with water. This research provides an enabling material to develop environmental-friendly and recyclable soft robots, reducing their negative environmental impact.

* Corresponding author.
E-mail address: cr@cqu.edu.cn (R. Chen).

https://doi.org/10.1016/j.matdes.2023.111783
0264-1275/

1. Introduction

Soft robots, made of soft materials, such as silicone rubbers,[1–3] polydimethylsiloxane (PDMS),[4] and other polymers,[5–9] have received extensive attention in various fields, such as bionic locomotion,[10–11] human-robot interactions,[12] and advanced medical devices.[13] They can interact with fragile objects without causing damage.[14] However, after working in an unstructured environment for a long time, soft robots will show performance degradation or even failure due to the weak mechanical properties of soft materials. In addition, after disposal at the end of their service life, these robots are difficult to be repaired and recycled,[15] generating significant environmental concern due to their non-degradability.[16].

Recently, researchers proposed to develop self-healable,[17–24] recyclable[25–27] or degradable soft robots.[28–29] For example, Terryn et al. proposed a soft pneumatic robot composed of Diels-Alder polymers and explored its self-healing ability.[30] Liu Z et al. fabricated a self-healable and recyclable starfish robot using tetraarylsuccinonitrile-liquid crystal elastomers.[31] Baumgartner et al. used gelatin, glycerol, citric acid, and sugar syrup to create an elastic and degradable bio-gel polymer for soft robots.[32] Zhang et al. proposed a self-healable, recyclable, and degradable flame-retardant gelatin-based bio-gel coating.[33] However, few materials can simultaneously possess all three properties—self-healing, recyclability, and safe degradability. Most existing soft materials can achieve long service life through self-healing and recycling. However, few materials can have regeneration and degradation capabilities. This is because the degradable materials exhibit poor mechanical properties;[28] adding degradability to renewable materials will reduce their mechanical properties,[32] making it challenging to meet the actuation requirements in soft robots. This limits the potential of soft robots to be environmental-friendly.

In this paper, a self-healable, recyclable, and degradable soft material (SRDSM) is reported that can be used for constructing robust soft robots with long service life and completely degraded (Fig. 1). The mechanical properties of the SRDSM can recover to 90 % of its original state after self-healing and 95 % after recycling. The degradability of the SRDSM is also demonstrated in water. Soft grippers, as the most common application in soft robots, have great potential for industrial applications with complete interaction and good flexibility. The cable-driven actuator is commonly used in soft grippers, and its higher strength and flexibility can well match the deformation capacity of soft grippers. Therefore, a cable-driven soft robotic gripper is designed and prototyped with the SRDSM. Experimental results show that the soft robots made of the SRDSM have unique self-healing, degradability, and recyclability advantages, enabling their extended service life and completely decomposable processing after service. The emerging SRDSM will promote the transition of soft robots from lab research to industrial applications in the future.

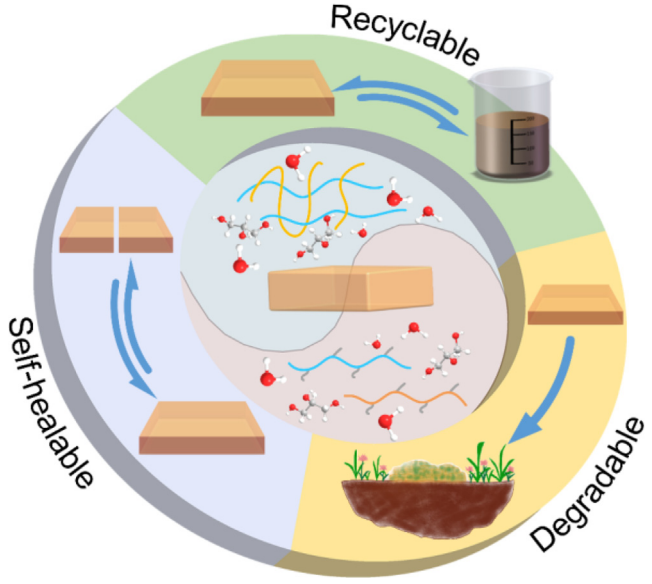

Fig. 1. The key properties of the new SRDSM.

2. Materials and methods

Materials: Gelatin (CP grade), glycerol (AR grade), and the rose-red B dye were purchased from Sinopharm Chemical Reagent Co. ltd. Polyvinyl alcohol (PVA; DP = 1700 ± 50) was obtained from Shanghai Yingjia Industrial Development Co. ltd. DI water was obtained from Henan Xinyuan Technology Co. ltd. Ferric chloride hexahydrate ($FeCl_3{\cdot}6H_2O$; AR grade) was obtained from Guangdong Guanghua Sci-Tech Co. ltd. All the reagents were used as received without further purification. All solutions were prepared using deionized water.

Preparation of $FeCl_3$ solution (1.5 wt%.): 2.5 g $FeCl_3{\cdot}6H_2O$ was dissolved in 100 mL DI water and stirred until the solution became transparent. Let it stand for 30 min and then take 14 mL of $FeCl_3$ solution from the upper clear layer.

Fabrication of the SRDSM (Fig. 2a): The SRDSM was prepared based on a mass ratio of 2:5:10 for gelatin: PVA: glycerol with DI water and $FeCl_3$ solution (1.5 wt%.). The gelatin (16 g) was first dissolved in DI water (220 g) together with the glycerol (80 g), which needed 0.5 h for the gelatin to dissolve completely. Then, the mixed solution was stirred at 150–200 r min^{-1} in a 50 °C water bath for 0.5 h until it became transparent. Next, PVA (40 g) powder was added to the gelatin solution and stirred thoroughly at 150–200 r min^{-1} in a 90 °C water bath for 1 h to get a transparent and sticky PVA/Gel solution. Then, the prepared $FeCl_3$ solution (1.5 wt%. 14 mL) was mixed with the PVA/Gel solution and stirred at 150–200 r min^{-1} in a 90 °C water bath for 1 h to obtain the stock SRDSM solution. After degassing, the final SRDSM solution was poured into a mold to cure in an oven at 80 °C. The SRDSM is finally obtained after demolding at room temperature, which is soft and can be easily twisted, folded, and stretched (Fig. 2b).

Water content measurement: The SRDSM solution is poured into tensile molds to dry for 4, 5, 6, 7, and 8 h in an oven at 80℃. The SRDSM samples were cut into small pieces of 10 × 10 × 2 mm. The initial mass m_0 was recorded before drying, and the final mass m_1 was measured after drying in an oven at 100 °C until the mass of the sample no longer decreased. The water contents of the samples were calculated as $\Delta m/m_0$, where $\Delta m = m_0\text{-}m_1$ is the mass difference before and after drying.

Fabrication of test sample: Measured samples made by the SRDSM follow ASTM-D412 standards. In the fabrication process, the SRDSM are dried for 8 h to maintain the same mechanical properties, and the finished products are always kept in a sealed bag before being tested (At least 88 h of storage to ensure stable mechanical properties of the material).

Fabrication of soft actuator: The casting mold of the soft actuator is formed by 3D printing. The SRDSM solution is poured into the mold and lets sit for 1 h. Then it is put in an oven at 80 °C for drying until the material is completely solidified. Next, the material is placed in a room-temperature environment to cool for 1 h and then demolded. After that, nylon thread is inserted into the hole of the actuator, and then it is tied at the top of the actuator.

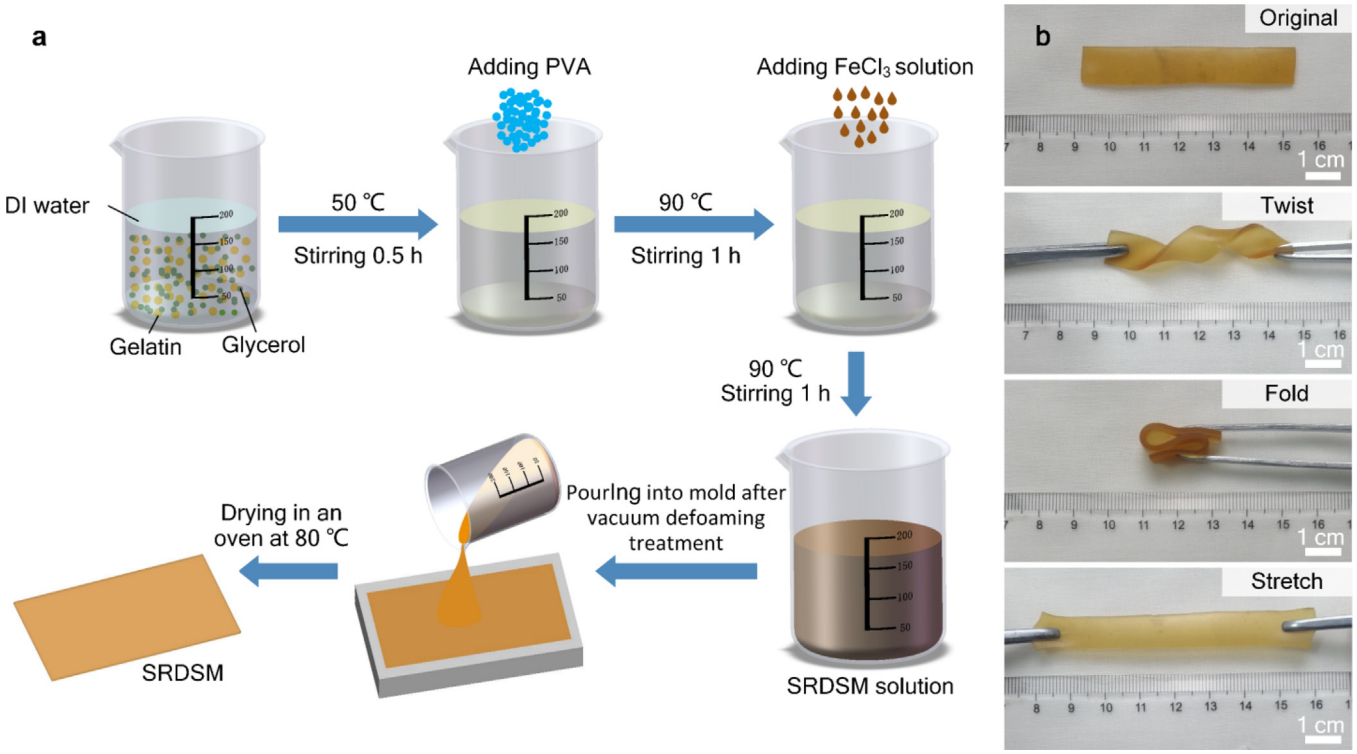

Fig. 2. The fabrication process and deformability of the SRDSM. (a) Schematic illustration of the fabrication process of the SRDSM. (b) Photographs of the deformed SRDSM samples when subjected to external loadings: twisting, folding and stretching.

Fabrication of soft gripper: Three as-fabricated soft actuators are assembled with three stepper motors(28BYJ-48), which are fixed on a 3D-printed chassis. The chassis is then mounted on the robotic arm. The movement of the actuators is driven by a motor, and the rotation of the motor is controlled by an 8051 microcontroller.

Measurement and characterization: The SEM images were obtained by a scanning electron microscope (TM4000Plus Ⅱ, Hitachi). The FTIR spectra were measured by an iS5 FT-IR spectrometer (Nicolet). The XRD measurements were carried out by an X-ray diffractometer (PANalytical X'Pert Powder, Spectris Pte. ltd) with a Cu source, operating at room temperature, 40 kV, and 40 mA current. The XPS images were obtained by X-ray photoelectron spectroscopy (ESCALAB 250Xi). Differential Scanning Calorimetry (DSC) tests were performed with a DSC 214 (NETZSCH) tester under nitrogen (N_2) protection at temperatures from −160℃ to 180℃ with a heating rate of 10℃ min^{-1}. Tensile tests were performed on an EZTest tensile testing machine (Shimadzu). Tensile stress–strain curves were measured at a stretching speed of 10 mm min^{-1}. The cyclic tensile test was done on the device MTS 858 Table Top System, which was loaded with a sine wave of frequency 1–5 Hz.

3. Results

The SRDSM has a firm and stable network structure [34] formed by gelatin and PVA (Fig. 3a and Supplementary Information 1). The gelatin molecular chains contain carboxyl (–COOH), amino ($–NH_2$) and hydroxyl groups (–OH) while PVA chains have –OH alcohol groups. With glycerol as a plasticizer, hydrogen bonds are formed between gelatin and PVA because hydrogen bonds are easier to form than the intramolecular or intermolecular bonds between gelatin and PVA.[35] In the literature,[36] Controlled experiments on gelatin-based gels with and without hydrogen bonding have shown that hydrogen bonding reduces the brittleness of gelatin-based gel materials. $FeCl_3$ solution will provide mobile iron ions (Fe^{3+}) to generate coordination cross-links with $–NH_2$, –OH, and –COOH. Since hydrogen bonds and metal coordination interactions are dynamically reversible non-covalent bonds, they will enable the self-healing properties of the SRDSM.[37–39] In addition, the SRDSM sample is observed to have a flat surface and homogeneous composition (Fig. 3b and Supplementary Information 2), indicating the excellent compatibility between gelatin and PVA in forming a uniform material.

The internal structure of the SRDSM is characterized by a Fourier transform infrared (FTIR) spectroscopy. The absorption peaks at 3282 cm^{-1} and 1418 cm^{-1} in the FTIR spectra of pure PVA are the characteristic hydroxyl peaks caused by stretching and bending vibrations, respectively (Fig. 3c). For pure gelatin, the absorption peaks at 1641 cm^{-1}, 1552 cm^{-1}, and 1239 cm^{-1} are caused by the amide Ⅰ (C═O), Ⅱ (N—H), and III (C—N) peaks of the protein [35], respectively. For comparison, a gelatin-PVA polymer is synthesized without $FeCl_3$. The peaks of amide I and III in the FTIR spectra of gelatin-PVA shift to 1650 cm^{-1} and 1260 cm^{-1}, respectively, while the peak of the amide Ⅱ disappears. Additionally, the peak of C—O stretching vibration shifts from 1100 cm^{-1} to 1104 cm^{-1}. This phenomenon indicates the hydrogen bonds formed between PVA and gelatin[35]. On the contrary, the FTIR spectra of the SRDSM show a peak at 1540 cm^{-1}, indicating the amide Ⅱ peaks of the protein. The added Fe^{3+} competes with PVA and gelatin to form ligand bonds with non-metallic elements, thus reducing the number of hydrogen bonds. This bond change results in the shifts of all the characteristic peaks in the FTIR spectrum of the SRDSM to the right at 1245 cm^{-1}, 1417 cm^{-1}, 1540 cm^{-1}, 2917 cm^{-1}, and 3280 cm^{-1}, which indicate the successful synthesis of the SRDSM.

The presence of interactions is also confirmed by the XRD analysis of PVA, gelatin, and the SRDSM (Fig. 3d). The characteristic peak at 40.64872° of PVA exists in the XRD peaks of the SRDSM, thereby confirming the existence of PVA in the prepared SRDSM.

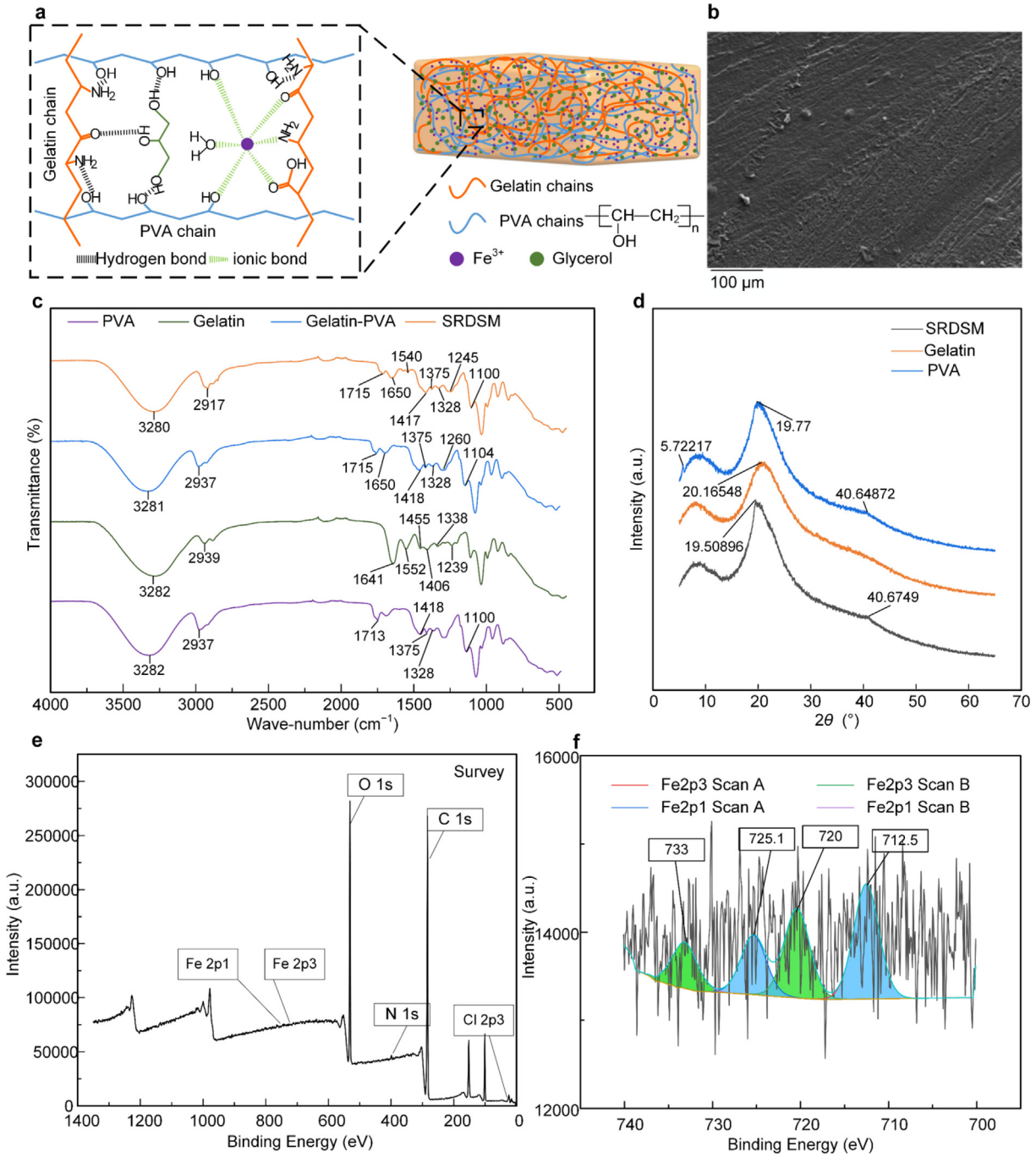

Fig. 3. Experimental characterization of the SRDSM. (a) Schematic diagram of the internal structure of the SRDSM. (b) SEM image of the SRDSM's cross-section. (c) Measured FTIR spectra for PVA, Gelatin, Gelatin-PVA, and the SRDSM. (d) X-ray diffractograms (XRD) of PVA, Gelatin, and the SRDSM. (e) Full spectrum of XPS for SRMSM. (f) Fitting spectra for XPS analysis of elemental Fe.

The characteristic peak at 19.79783° of PVA and the characteristic peak at 20.16548° of gelatin also exist in the XRD peaks of the SRDSM, which shift to 19.50896°, thereby confirming the existence of PVA and gelatin in the prepared SRDSM and the presence of interactions between PVA and gelatin.

The SRDSM carries out XPS tests to investigate the coordination state of Fe^{3+} ions. Due to the small amount of $FeCl_3$ added, only a little elemental Fe peak is shown in the full SRDSM spectrum (Fig. 3e). In contrast, four typical peaks (733 eV. 725.1 eV. 720 eV. 712.5 eV) are shown in the Fe 2p region of the single element spectrum (Fig. 3f), which can be attributed to the Fe (III) 2p 3/2 and Fe (III) 2p 1/2 electron configurations. The above experiments and data (Supplementary Information 3) show that the binding energy peak of Fe^{3+} (binding energy of Fe^{3+} and Cl^- coordination) from 730.2 eV, 725.2 eV, 717.5 eV, and 713.6 eV to 733 eV, 725.2 eV, 720 eV, and 712.5 eV(binding energy of Fe^{3+} in SRDSM), the peak value shifted to the right. And the higher the content of Fe^{3+}, the greater the intensity and binding energy. Indicating that

the interaction between Fe^{3+}, PVA, and gelatin chains leads to subtle changes in the molecular structure and that Fe^{3+} can produce metal coordination with $-NH_2$, –OH, and –COOH.

3.1. Mechanical properties and stability of the SRDSM

The mechanical properties of the SRDSM with different material ratios are characterized (Supplementary Information. 4). It can be seen that as the gelatin mass increases, the fracture strain and Young's modulus of the SRDSM decrease (Fig. 4a). When the gelatin: PVA ratio changes from 1:5 to 2:5, the fracture stress of the SRDSM slightly increases from 3.85 MPa to 3.94 MPa, and then decreases with the increase of the material ratio. This indicates that the polymer becomes softer and weaker with more gelatin added. On the other hand, the fracture strain, fracture stress, and Young's modulus of the SRDSM increase as the PVA ratio increases (Supplementary Information. 5), which indicates that more PVA can improve the fracture strength of the SRDSM. This phenomenon is because PVA is a linear crystalline polymer with good tensile properties, while gelatin is more brittle. Thus, a higher ratio of gelatin will reduce the tensile properties of the SRDSM, and a high percentage of PVA will lead to better stretchability of the SRDSM.

Based on the tensile testing, it can be seen that the mechanical properties of the SRDSM are related to the gelatin, PVA, and glycerol concentration. When the ratio of glycerol: PVA changes from 1:1 to 5:1, the fracture stress of the SRDSM first increases, then keeps almost as constant, and finally decreases (Supplementary Information. 6). It is found that the fracture strain of the SRDSM increases while Young's modulus of the SRDSM decreases as the percentage of glycerol increases. Thus, the mechanical properties of the SRDSM can be tuned by adjusting the percentages of each component according to the specific requirements for different applications. For example, for soft robots, Young's modulus in the range of 0.1 MPa-10 MPa is desirable[32]. Therefore, the specific

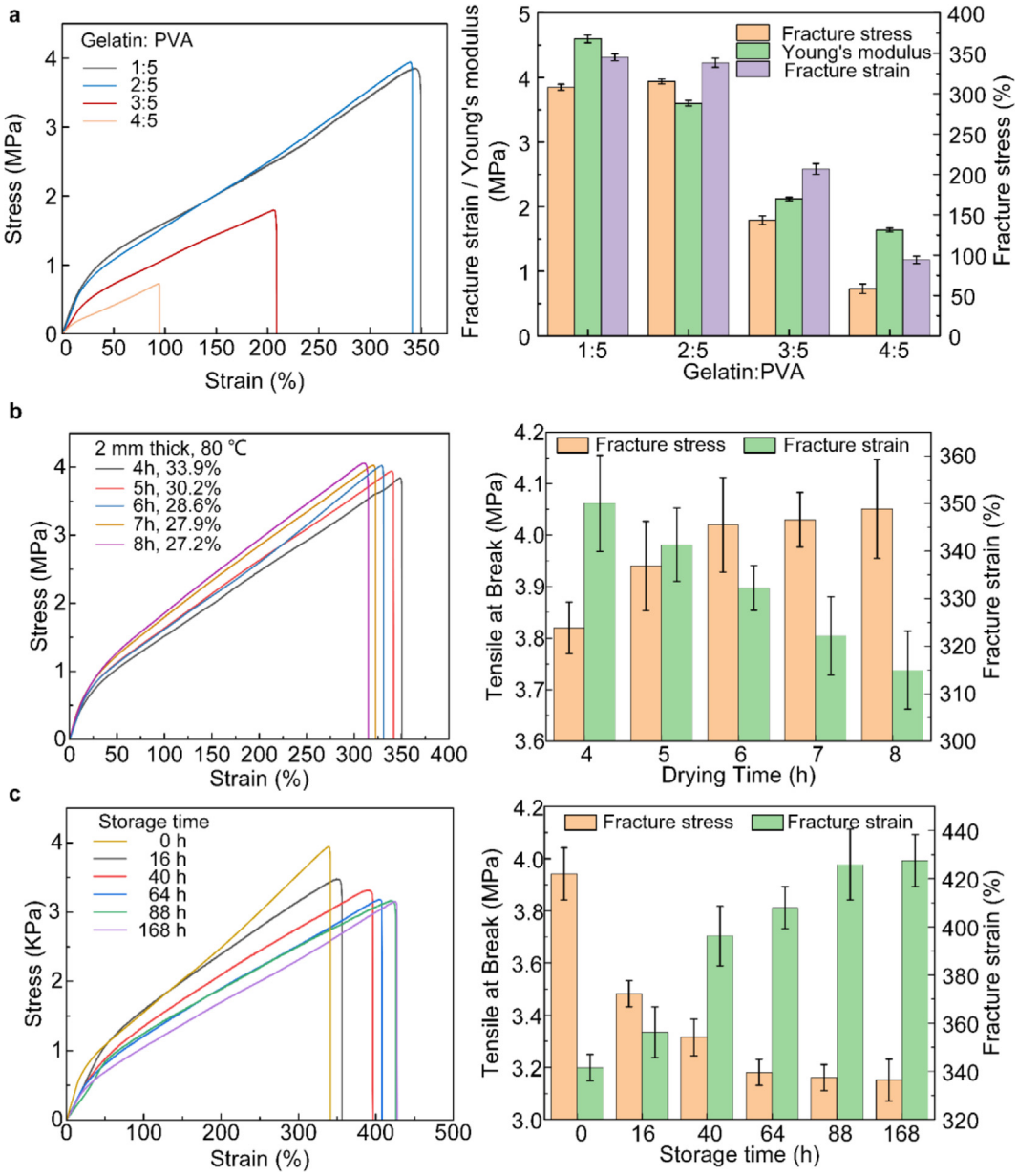

Fig. 4. Mechanical properties of the SRDSM. (a) Stress–strain curves of the SRDSMs with different gelatin: PVA ratios. (b) Stress–strain curves of the SRDSMs under drying times show fracture strain and fracture stress for different drying times. (c) Tensile test results of the SRDSMs after being placed in an ambient environment for different time (0 h, 16 h, 40 h, 64 h, 88 h, 168 h), show fracture strain and stress of the SRDSM after being placed in a room-temperature environment for 0, 16, 40, 64, 88 and 168 h.

ratio of 2:5:10 for gelatin: PVA: glycerol will be used for the SRDSM in the following experimental study.

The water content in the SRDSM varies with the drying time. After the fresh prepared SRDSM has a water content of 55 %. When the drying time increases from 4 h to 8 h, the water content of the SRDSM reduces from 33.9 % to 27.2 %, leading to a change of the mechanical properties (Fig. 4b). In addition, as the drying time increases, the fracture stress of the material gradually increases from 3.81 MPa to 3.94 MPa while the fracture strain gradually decreases from 350.25 % to 314.91 %. These results indicate that the decreased water content in the SRDSM causes a reduction of its fracture strain and an increase in its fracture stress.

When the SRDSM is removed from the oven and placed in the environment, it will absorb water from the environment through hydrodynamic equilibrium. The moisture absorption ratio m_a/m_i can be calculated based on the mass m_a measured after moisture absorption and the initial mass m_i. It is found that for the SRDSM with the same water content (19 %) at the temperature of 25℃, the SRDSM absorbs moisture faster in an environment with higher relative humidity (RH) before reaching equilibrium (Supplementary Information. 7). For the same temperature and RH environment (25℃, 62 % RH), the SRDSM with a lower water content will have a larger moisture absorption rate before reaching equilibrium (Supplementary Information. 8). Stored at the same environment (25℃, 62 % RH) for 16, 40, 64, 88 and 168 h, the water content of the SRDSM changes from 30.2 % to 37.60 %, 40.61 %, 42.70 %, 43.65 %, and 43.63 % respectively. Meanwhile, the fracture strain of the SRDSM gradually decreases and the fracture stress gradually increases. After 88 h, the fracture strain and fracture stress do not change anymore (Fig. 4c). When the water content of the SRDSM increases from 30.20 % to 43.63 %, the fracture strain increases from 341.55 % to 427.61 %, and the fracture stress reduces from 3.94 MPa to 3.15 MPa. With the increased water content, the elongation at break increases slightly while the strength at break decreases slightly. The SRDSM is suitable for fabricating soft robots regardless of the mechanical properties change. To test the stability and service life of the SRDSM at room temperature, the SRDSM is tested in cyclic tension (Supplementary Information. 9). The experimental data showed that SRDSM can be used for a long time in the strain range of 150 % to 300 %. When the SRDSM was strained at 150 % in the experiment, it could be effectively cyclically stretched 100,000 times and still did not break; when the SRDSM was strained at 300 % in the experiment, it could still be effectively cyclically stretched 20,000 times; demonstrating the good stability and service life of the material. At the same time, with the increase of loading times and loading time, the length of the material will have a linear plastic deformation. But not beyond the use of the demand range (Supplementary Information. 10). Therefore, the SRDSM can be considered reliable and stable in a room-temperature environment.

3.2. Self-healing, recyclability, and degradability of the SRDSM

Soft materials with repairability, such as self-healing capabilities and recyclability, have a longer service life than those materials without such properties. The hydrogen bonds and metal ion coordination interactions in the SRDSM are dynamically reversible, enabling the SRDSM's self-healing capabilities and recyclability. Fig. 5a shows the self-healing process of the SRDSM. Two requirements must be met during the healing process to ensure a firmly bonded interface: the two fractured surfaces are compressed tightly, and sufficient hydrogen bonds and metal coordination interactions are restored. When heated in an oven under 85℃, which is in the molten region of the SRDSM (Supplementary Information. 11), the SRDSM sample absorbs thermal energy, and the fracture interfaces are melted. As a result, the mobility of the SRDSM's polymer chains on the fracture interfaces increases. The gap between the two interfaces is filled, and new hydrogen and metal coordination bonds will be formed. Long-time curing in the oven will further break more chains, increase the material's mobility, and provide sufficient time for the fracture interfaces to heal. After that, the sample is cooled down to 25℃ to reduce the movement of the molecular chains and achieve stable new hydrogen bonds and metal coordination interactions. After the two pieces of the SRDSM (one piece is dyed pink) are healed together, the SRDSM film can undergo deformations under stretching (Fig. 5b). At the same time, to demonstrate the influence of Fe^{3+} on the healing effect, the samples with and without Fe^{3+} are prepared, and the controlled healing experiment is carried out (Supplementary Information. 12). The results show that Fe^{3+} added in the healing process of the material would make the Fe^{3+} interact with more –OH to produce coordination bonds, so as to achieve better healing effect.

The recovery of the SRDSM's mechanical properties is characterized by the self-healing recovery efficiency (RE), as defined by the fracture stress $RE_1 = S_h/S_o$ and the fracture strain $RE_2 = S_{he}/S_{or}$, where the S_h, S_o, S_{he}, and S_{or} are the fracture stress after healing, the original fracture stress, the fracture strain after healing and the original fracture strain, respectively. These parameters are acquired after the sample's water content stabilizes (42.5 %-43.6 %) in the ambient environment (25℃, 62 % RH). The influences of heating temperature and time on the self-healing RE of the SRDSM are studied. When the SRDSM is cured at 55 °C, 65 °C, 75 °C, and 85 °C for 5 h, the fracture strain and stress after self-healing gradually increase with the temperature (Fig. 5c). The fracture strain and stress REs of the sample at 85℃ can reach 90.4 % and 85.9 %, respectively. The fracture strain and stress are also improved after a longer heating time (Fig. 5d). With the heating time increasing from 1 h to 5 h, the fracture strain and stress recovery rates increase from 45.6 % to 90.4 % and 42.9 % to 85.9 %, respectively. Therefore, a higher heating temperature and longer heating time can increase the self-healing RE of the SRDSM. This can be explained by the fact that under a higher temperature for a longer time, the movement of SRDSM's molecular chains on the fracture surfaces increases, thereby forming more new hydrogen bonds and metal coordination interactions.

When the SRDSM is severely damaged, such as irreparably deformed or losing its original function, it can be recycled to produce new products (Fig. 5e). For example, the broken material can form a five-pointed star or rectangular shape product. Experimental results show that after recycling five times, the fracture strain and fracture stress of the SRDSM can recover 95.8 % and 97.3 % of its original values (Fig. 5f). The recovery capability is attributed to the reformation of dynamic hydrogen bonds and metal coordination interactions in the material. The SRDSM is water-soluble, and the hydrogen bonds and metal coordination interactions in the SRDSM can be broken and accelerated by heating. However, as the solved SRDSM is cast and dried, new bonds will form to restore its mechanical properties. The recyclability of the SRDSM enables it to be used for multiple times, thereby prolonging its service life and saving resources.

The degradation time of the SRDSM in water increases as the volume of the SRDSM increases (Supplementary Information. 13). The degradation time of the SRDSM samples with a dimension of 20 × 20 × 1 mm in 1000 mL of DI water at 95℃ is approximately 44 min (Fig. 5g). The degradation time increases to 40 h in 1000 mL of DI water at 25℃ (Fig. 5h). The pH, suspended solids (SS), and the chemical oxygen demand (COD) are 6.5, 27.73 mg/L, and 68.054 mg/L, respectively (GB 8978–1996, secondary standard: pH: 6–9; SS, 150 mg/L; COD, 150 mg/L). This result means after the degradation of the material, and the obtained solution can

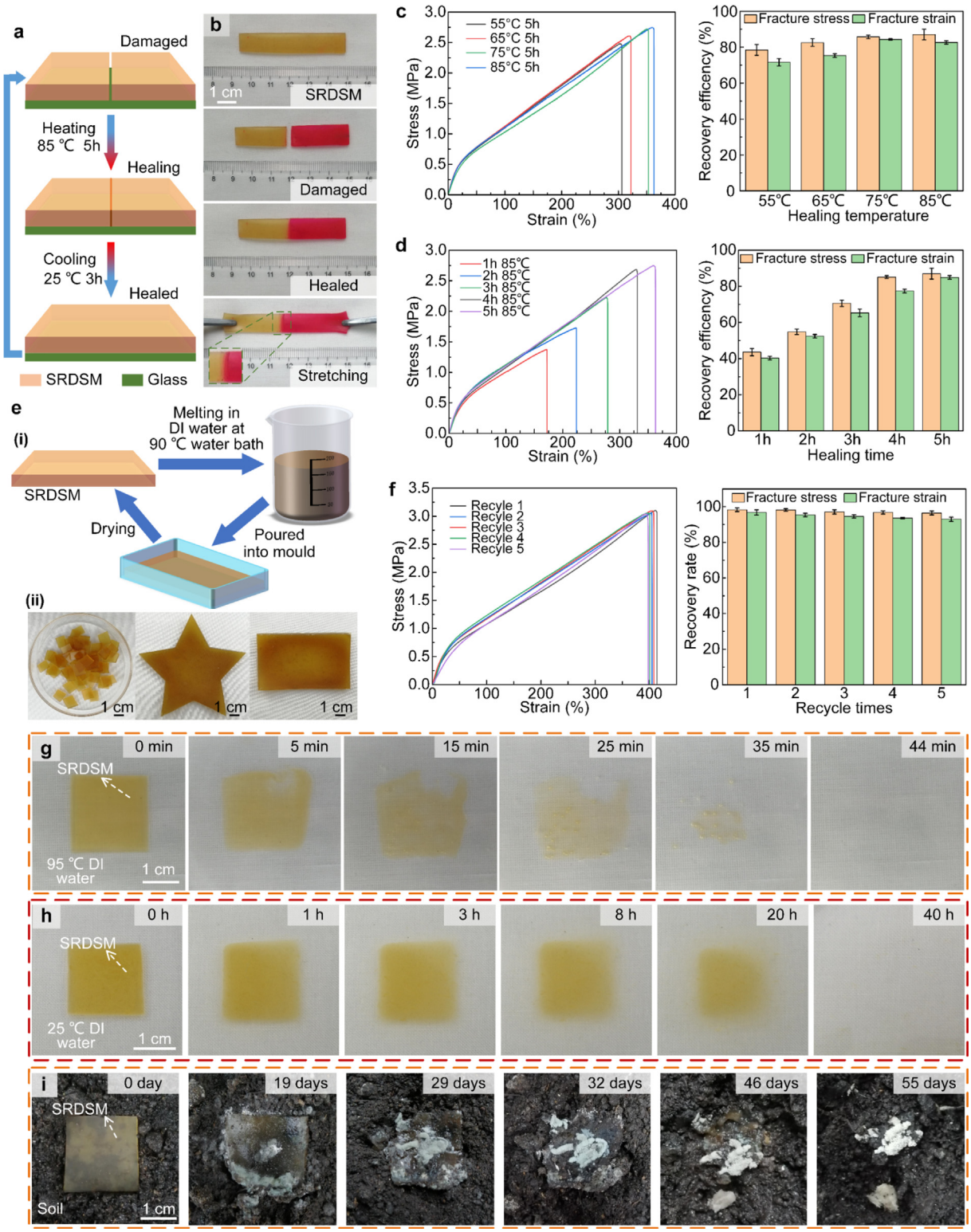

Fig. 5. The SRDSM's self-healing and recycling properties. (a) The healing process of the SRDSM. (b) Photos of the SRDSM before and after self-healing. (c) Tensile test results of SRDSMs with the same healing time and different healing temperatures. (d) Tensile test results of the SRDSMs with the same healing temperature and different healing times. (e) (i) The recycling process of the SRDSM. (ii) The initial SRDSM after recycling into a star shape and a rectangular shape. (f) Tensile test results of the SRDSMs with different recycle times and the recovery rate of fracture stain and fracture stress of the SRDSMs with different recycle times. (g) The SRDSM decomposed in 95 ℃ DI water. (h) The SRDSM decomposed in 25 ℃ DI water. (i) The SRDSM degrading in soil.

meet emission standards, that is, the material can be degraded completely. In addition, the SRDSM will take 33 days to degrade in the soil (Fig. 5i). The SRDSM is easily affected by temperature in water, resulting in the breakdown of hydrogen bonds and decomposition into various components. The higher the temperature, the faster the decomposition rate of SRDSM and the faster the dissolution rate of components. Therefore, the disappearance of SRDSM in water mainly involves decomposition and degradation

processes. The decomposition process is mainly affected by temperature, while the degradation is mainly affected by microorganisms and enzymes [32] (Fig. 5g&5h and Supplementary Information. 14). With the SRDSM degraded completely, the material can be decomposed without specific treatment or processing after being discarded.

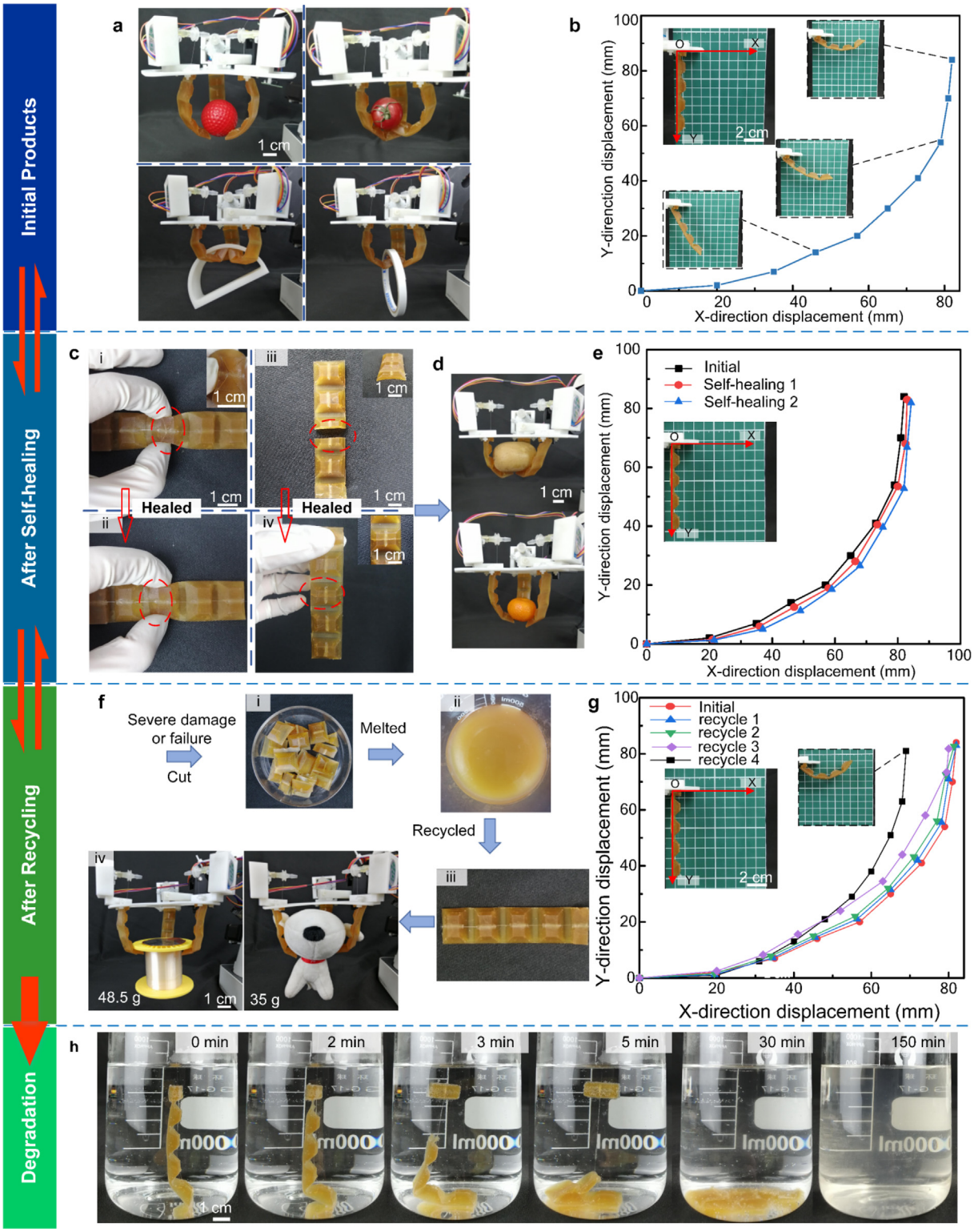

Fig. 6. Demonstration of the Soft gripper made of the SRDSM. (a) Grasping a golf ball, a tomato, a 3D printed mold, and a tape. (b) The bending profile of the finger actuator. (c) A soft actuator with a 1 mm deep cross-shaped wound can recover after self-healing (i. ii), and a completely cut-off soft actuator can also recover after self-healing (iii. iv). (d) Grasp a kiwi fruit by a soft gripper self-healed once and grasp an orange by the gripper self-healed twice. (e) The trajectory of the tip of the original actuator, the actuator that healed once, and the twice-healed actuator. Photographs of the severed soft actuator before and after self-healing. (f) Recycling a soft actuator and demonstrating the recycled gripper for grasping a toy and a coil bobbin. (g) The trajectory of the tip of the original actuator and the once-, twice-, and three-times recycled actuator. (h) The decomposition process of the soft actuator in 90℃ DI water. (For interpretation of the references to colour in this figure legend, the reader is referred to the web version of this article.)

3.3. Evaluation of the soft robotic gripper made of the SRDSM

The developed SRDSM can be utilized to fabricate soft robots capable of self-healing, recycling, and degradation. A cable-actuated soft gripper (Supplementary Information. 15) is demonstrated to grasp objects of different sizes and shapes (Fig. 6a and Supplementary Movie 1). As shown in Fig. 6b, the bottom of the gripper finger is fixed on the substrate and the finger body can bend freely under the actuation of the cable driven by a DC motor (Supplementary Information. 16). A finite element model is built to calculate the strain distribution of the soft finger (Supplementary Information. 17 and 18). The maximum bending force was measured by placing a load cell on the tip of the finger in the initial state. The maximum vertical force is around 0.6 N.

The gripper can be used in unknown and dynamic situations with possible sharp tips. It is demonstrated that minor superficial wounds (cuts and abrasions) or fractures have little impact on the grasping performance of the gripper. As the number of uses increases, the concentrated stress on the wounds will increase, causing wounds to grow and damage their grasping stability. In severe cases, a fracture wound can cause complete failure of grasping operations. Therefore, self-healing will be essential to restore its performance. The self-healing process of the SRDSM can be achieved through a thermal heating process. As shown in Fig. 6c, a 1 mm deep cross-shaped wound is cut on the surface of one finger-like actuator by a scalpel. Then, to heal the actuator, the two surfaces of the wound are pressed together tightly and placed in an oven at 85℃ for 5 h to let the hydrogen bonds and metal coordination interactions reform along the cut surfaces (Fig. 6c(ii)). It also works for a completely cut-off finger along the cross-section (Fig. 6c(iii)-(iv)). After the self-healing procedure, the wounds are completely healed, almost invisible, and the actuators can work well again to perform grasping tasks, such as picking up a kiwi fruit or an orange (Fig. 6d). It is also used to manipulate a golf ball (Supplementary Movie 2) after the first and second healing. In addition to healing damages, it is crucial to restore the mechanical performance of the actuator after the self-healing process. Therefore, the actuator's bending performance is also evaluated after self-healing repair. This damage-healing cycle is repeated three times. It is found that the finger's bending profile shows a little variation (Fig. 6e) and the mechanical performance of the bending actuator is nearly completely restored after each damage-healing test cycle.

When a gripper is completely destroyed into small pieces, the self-healing process may not be applicable due to the impossible to form a tight contact between surfaces. Thus, they can be recycled to make a new gripper, which completely restores its initial shape and mechanical properties. To demonstrate the recyclability of the gripper, one finger actuator was cut into small pieces (Fig. 6f) and then dissolved it in DI water to form an SRDSM solution. The solution was poured into a mold to fabricate a new actuator (Fig. 6f). The remanufactured gripper from the recycled SRDSM can keep its grasping ability well, such as picking up a toy and a coil bobbin (Fig. 6f(iv)). This recycling-fabrication process is repeated four times, and find that the fingers' motion trajectories slightly shift upward after recycling, while the bending force at the tip is tested to be 0.6 N after the fourth recycling (Fig. 6g). Finally, a soft finger-shaped actuator is placed in deionized water at 90 °C to verify its degradability. As shown in Fig. 6h, the soft actuator completely dissolves after 150 min, remaining a transparent solution. The self-healing ability and recyclability of the SRDSM enable the soft actuator to have a longer service life, and its degradability prevents it from generating possible pollution at its end of life. This SRDSM-based soft actuator can be used to develop various soft robots, such as soft crawling robots, auxiliary medical devices, and smart wearable devices capable of recycling, self-healing, and degradation.

4. Conclusions

A new SRDSM is developed to fabricate a soft gripper successfully. The SRDSM is formed with hydrogen bonds and metal coordination interactions. It is self-healable, recyclable, and degradable and can survive under fracture stress of 3–4 MPa. Therefore, SRDSM can be used as a high-quality material in soft robot fields under medium–low loads. The mechanical properties of the SRDSM can be tuned by changing the material composition ratio during the synthesis process and be affected by the drying time. It is demonstrated that the SRDSM can be self-healed by heating the fractured parts to 85℃ in an oven to recover its mechanical properties. The recycled SRDSM based on a simple molten solvent casting-heating procedure showed little reduction in its mechanical properties after five recycling-fabrication cycles. When the SRDSM-based soft robots are retired or fail at the end of their service life, the soft components can degrade completely. The possible applications of the SRDSM in soft robots are demonstrated. A cable-driven gripper made of the SRDSM exhibited excellent grasping capability after healing and recovery, and the gripper fingers can degrade completely. The SRDSM will provide a new solution to develop versatile, environmental-friendly soft robots for different kinds of applications.

CRediT authorship contribution statement

Rui Chen: Conceptualization, Methodology, Funding acquisition, Project administration, Supervision, Writing – original draft, Writing – review & editing. **Xin Li:** Conceptualization, Methodology, Investigation, Project administration, Writing – review & editing. **Qin Xiong:** Conceptualization, Methodology, Writing – review & editing. **Xinyu Zhu:** Conceptualization, Writing – review & editing. **Huigang Wang:** Conceptualization, Writing – review & editing. **Wenbiao Wang:** Writing – review & editing. **Guanjun Bao:** Writing – review & editing. **Zhen Chen:** Writing – review & editing. **Changyong (Chase) Cao:** Writing – review & editing. **Jun Luo:** Writing – review & editing.

Data availability

Data will be made available on request.

Declaration of Competing Interest

The authors declare that they have no known competing financial interests or personal relationships that could have appeared to influence the work reported in this paper.

Acknowledgments

We thank Dr. Jianglong Guo who is currently working at Harbin Institute of Technology (Shenzhen) and Dr. Jonathon Rossiter who is currently working at the University of Bristol for their suggestions to revise the article.

Funding

National Key Research and Development Project of China (grant no. 2020YFB1313000)

National Natural Science Foundation of China (grant no. 52075051)

Natural Science Foundation of Chongqing, China (grant no. cstc2021jcyj-msxmX0908)

Fundamental Research Funds for the Central Universities (grant no. 2021CDJQY-015)

Appendix A. Supplementary material

Supplementary data to this article can be found online at https://doi.org/10.1016/j.matdes.2023.111783.

References

[1] G. Agarwal, N. Besuchet, B. Audergon, J. Paik, Stretchable Materials for Robust Soft Actuators towards Assistive Wearable Devices, Sci. Rep. 6 (2016) 1–8.
[2] R.V. Martinez, C.R. Fish, X. Chen, G.M. Whitesides, Elastomeric Origami: Programmable Paper-Elastomer Composites as Pneumatic Actuators, Adv. Funct. Mater 22 (2012) 1376–1384.
[3] C. Larson, B. Peele, S. Li, S. Robinson, M. Totaro, L. Beccai, B. Mazzolai, R. Shepherd, Highly Stretchable Electroluminescent Skin for Optical Signaling and Tactile Sensing, Nature 351 (2016) 1071–1074.
[4] J. Lessing, S.A. Morin, C. Keplinger, A.S. Tayi, G.M. Whitesides, Stretchable Conductive Composites Based on Metal Wools for Use as Electrical Vias in Soft Devices, Adv. Funct. Mater 25 (2015) 1418–1425.
[5] J. Cao, L. Qin, J. Liu, Q. Ren, C.C. Foo, H. Wang, H.P. Lee, J. Zhu, Untethered Soft Robot Capable of Stable Locomotion Using Soft Electrostatic Actuators, Extreme Mech. Lett. 21 (2018) 9–16.
[6] J. Shintake, S. Rosset, B. Schubert, D. Floreano, H. Shea, Versatile Soft Grippers with Intrinsic Electroadhesion Based on Multifunctional Polymer Actuators, Adv. Mater. 28 (2016) 231–238.
[7] F. Ongaro, S. Scheggi, C.K. Yoon, F. Brink, S.H. Oh, D.H. Gracias, S. Misra, Autonomous planning and control of soft untethered grippers in unstructured environments, Micro-Bio Robot 12 (2017) 45–52.
[8] A.M. Hubbard, R.W. Mailen, M.A. Zikry, M.D. Dickey, J. Genzer, Controllable Curvature from Planar Polymer Sheets in Response to Light, Soft Matter 13 (2017) 2299–2308.
[9] E. Diller, M. Sitti, Three-Dimensional Programmable Assembly by Untethered Magnetic Robotic Micro-Grippers, Adv. Funct. Mater 24 (2014) 4397–4404.
[10] A.D. Marchese, C.D. Onal, D. Rus, Autonomous soft robotic fish capable of escape maneuvers using fluidic elastomer actuators, Soft Robot 1 (2014) 75–87.
[11] M. Wehner, R.L. Truby, D.J. Fitzgerald, B. Mosadegh, G.M. Whitesides, J.A. Lewis, R.J. Wood, An integrated design and fabrication strategy for entirely soft, autonomous robots, Nature 536 (2016) 451–455.
[12] P. Polygerinos, Z. Wang, K.C. Galloway, R.J. Wood, C.J. Walsh, Soft robotic glove for combined assistance and at-home rehabilitation, Robot. Auton. Syst 73 (2015) 135–143.
[13] C. Lee, W.J. Park, M. Kim, S. Noh, C. Yoon, C. Lee, Y. Kim, H.H. Kim, H.C. Kim, S. Kim, Pneumatic-type surgical robot end-effector for laparoscopic surgical-operation-by-wire, Biomed. Eng. Online 13 (2014) 1–19.
[14] F. Ilievski, A.D. Mazzeo, R.F. Shepherd, X. Chen, G.M. Whitesides, Soft Robotics for Chemists, Angew. Chem 123 (2011) 1930–1935.
[15] A.J. Partridge, H.Y. Chen, N.H. Le, C. Xu, H. Eichorn, E. Pulvirenti, A. Manzini, A.T. Conn, J. Rossiter, ReRobot: Recycled Materials for Trustworthy Soft Robots, Soft Robot. (2022) 148–153.
[16] F. Hartmann, M. Baumgartner, M. Kaltenbrunner, Becoming sustainable, the new frontier in soft robotics, Adv. Mater 33 (2021) 2004413.
[17] F. Jiang, Z. Zhang, X. Wang, G. Cheng, Z. Zhang, J. Ding, Pneumatically Actuated Self-Healing Bionic Crawling Soft Robot, Intell. Robot. Syst. 100 (2020) 445–454.
[18] E. Roels, S. Terryn, J. Brancart, R. Verhelle, G.V. Assche, B. Vanderborght, Additive Manufacturing for Self-Healing Soft robotics, Soft Robot. 7 (2020) 711–723.
[19] S. Terryn, G. Mathijssen, J. Brancart, D. Lefeber, G.V. Assche, B. Vanderborght, Development of a self-healing soft pneumatic actuator: a first concept, Bioinspir. Biomim 10 (2015) 046007.
[20] E. Borré, J.F. Stumbé, S. Bellemin-Laponnaz, M. Mauro, Light-Powered Self-Healable Metallosupramolecular Soft Actuators, Angew. Chem. Int. Ed 55 (2016) 1313–1317.
[21] S. Terryn, J. Brancart, D. Lefeber, G. V. Assche, B. Vanderborght, A Pneumatic Artificial Muscle Manufactured Out of Self-Healing Polymers That Can Repair Macroscopic Damages, IEEE Robot. Autom. Lett. PP (2017) 1–1.
[22] T.J. Wallin, J.H. Pikul, S. Bodkhe, B.N. Peele, B.C. Mac Murray, D. Therriault, B.W. McEnerney, R.P. Dillon, E.P. Giannelis, R.F. Shepherd, Click Chemistry Stereolithography for Soft robotics that Self-Heal, Mater. Chem. B 5 (2017) 6249–6255.
[23] S. Terryn, E. Roels, J. Brancart, G.V. Assche, B. Vanderborght, Room Temperature Self-Healing in Soft Pneumatic Robotics: Autonomous Self-Healing in a Diels-Alder Polymer Network, IEEE Robot. Autom. Mag 27 (2020) 44–55.
[24] R.F. Shepherd, A.A. Stokes, R.M.D. Nunes, G.M. Whitesides, Soft Machines That are Resistant to Puncture and That Self Seal, Adv. Mater 25 (2013) 6709–6713.
[25] J. Shintake, H. Sonar, E. Piskarev, J. Paik, D. Floreano, Soft Pneumatic Gelatin Actuator for Edible Robotics, Intell Robot Syst (2017) 6221–6226.
[26] Z. Jiang, M.L. Tan, M. Taheri, Q. Yan, T. Tsuzuki, M.G. Gardiner, B. Diggle, L.A. Connal, Strong, Self-Healable, and Recyclable Visible-Light-Responsive Hydrogel Actuators, Angew. Chem 18 (2020) 7115–7122.
[27] Y. Zhu, J. Zhang, Q. Wu, M. Chen, G. Huang, J. Zheng, J. Wu, Three-Dimensional Programmable, Reconfigurable, and Recyclable Biomass Soft Actuators Enabled by Designing an Inverse Opal-Mimetic Structure with Exchangeable Interfacial Crosslinks, ACS Appl. Mater. Interfaces 12 (2020) 15757–15764.
[28] S. Walker, J. Rueben, T.V. Volkenburg, S. Hemleben, C. Grimm, J. Simonsen, Y. Mengüç, Using an environmentally benign and degradable elastomer in soft robotics, Int J Intell Robot Appl 1 (2017) 124–142.
[29] Y. Bar-Cohen, F. Vidal, J. Rossiter, J. Winfield, I. Ieropoulos, Here today, gone tomorrow: biodegradable soft robots, Electroactive Polymer Actuators and Devices (2016) 312–321.
[30] S. Terryn, J. Brancart, D. Lefeber, V. G. Assche, B. Vanderborght, Self-healing soft pneumatic robots, Sci. Robot, 2 (2017) eaan4268.
[31] Z. Liu, H.K. Bisoyi, Y. Huang, M. Wang, H. Yang, Q. Li, Thermo- and Mechanochromic Camouflage and Self-Healing in Biomimetic Soft Actuators Based on Liquid Crystal Elastomers, Angew Chem Int Ed Engl 61 (2022) e202115755.
[32] M. Baumgartner, F. Hartmann, M. Drack, D. Preninger, D. Wirthl, R. Gerstmayr, L. Lehner, G. Mao, R. Pruckner, S. Demchyshyn, L. Reiter, M. Strobel, T. Stockinger, D. Schiller, S. Kimeswenger, F. Greibich, G. Buchberger, E. Bradt, S. Hild, S. Baue, M. Kaltenbrunner, Resilient yet entirely degradable gelatin-based biogels for soft robotics and electronics, Nat. Mater 19 (2020) 1102–1109.
[33] L. Zhang, Y. Huang, P. Sun, Y. Hai, S. Jiang, A self-healing, recyclable, and degradable fire-retardant gelatin-based biogel coating for green buildings, Soft Matter 17 (2021) 5231–5239.
[34] J.P. Gong, Y. Katsuyama, T. Kurokawa, Y. Osada, Double-Network Hydrogels with Extremely High Mechanical Strength, Adv. Mater 15 (2003) 1155–1158.
[35] S.M. Pawde, K. Deshmukh, S. Parab, Preparation and Characterization of Poly (vinyl alcohol) and Gelatin Blend Films, Appl. Polym. Sci 109 (2008) 1328–1337.
[36] P. Bergo, P.J.A. Sobral, Effects of plasticizer on physical properties of pigskin gelatin films, Food Hydrocoll. 21 (2007) 1285–1289.
[37] X. Yan, Q. Chen, L. Zhu, H. Chen, D. Wei, F. Chen, Z. Tang, Jia. Yang, J. Zheng, High Strength and Self-Healable Gelatin/Polyacrylamide Double Network Hydrogels, Mater. Chem. B, 5 (2017) 7683-7691.
[38] Z. Wei, J. He, T. Liang, H. Oh, J. Athas, Z. Tong, C. Wang, Z. Nie, Autonomous Self-Healing of Poly (Acrylic Acid) Hydrogels Induced by the Migration of Ferric ions, Polym. Chem 4 (2013) 4601–4605.
[39] Y. Wang, J. Yan, Z. Wang, J. Wu, G. Meng, Z. Liu, X. Guo, One-pot fabrication of triple-network structure hydrogels with high-strength and self-healing properties, Mater. Lett 207 (2017) 53–56.